

PAPER • OPEN ACCESS

## Gyromagnetic nonlinear transmission line generator of high voltage pulses modulated at 4 GHz frequency with 1000 Hz pulse repetition rate

To cite this article: M R Ulmasculov *et al* 2017 *J. Phys.: Conf. Ser.* **830** 012027

View the [article online](#) for updates and enhancements.

### Related content

- [Volume Diffuse Dielectric Barrier Discharge Plasma Produced by Nanosecond High Voltage Pulse in Airflow](#)  
Qi Haicheng, Gao Wei, Fan Zhihui et al.
- [Measurements of EHD flow patterns in ESP with DC+Pulsed voltage hybrid power supply](#)  
Janusz Podliski, Marek Kocik and Jerzy Mizeraczyk
- [A nanosecond kilovolt pulse generator using microstrip charging lines](#)  
A R Waugh



**IOP | ebooks™**

Bringing you innovative digital publishing with leading voices to create your essential collection of books in STEM research.

Start exploring the collection - download the first chapter of every title for free.

# Gyromagnetic nonlinear transmission line generator of high voltage pulses modulated at 4 GHz frequency with 1000 Hz pulse repetition rate

M R Ulmasculov, K A Sharypov, S A Shunailov, V G Shpak, M I Yalandin, M S Pedos and S N Rukin,

Institute of Electrophysics UB RAS, 620016, Ekaterinburg, Russian Federation

E-mail: marat@iep.uran.ru

**Abstract.** Results of testing of a generator based on a solid-state drive and the parallel gyromagnetic nonlinear transmission lines with external bias are presented. Stable rf-modulated high-voltage nanosecond pulses were shaped in each of the four channels in 1 s packets with 1000 Hz repetition frequencies. Pulse amplitude reaches -175 kV, at a modulation depth of rf-oscillations to 50 % and the effective frequency  $\sim 4$  GHz.

## 1. Introduction

Multichannel microwave sources [1-7] considerably increase a power flux density of rf-emission in the far-field region of the major maximum of the directional pattern (DP) and sharpen a beam [1-3]. Maximum increase in the flux power density is quadratic to a quantity of sources. So, it is clear that there is an interest in the systems when a power of every channel reaches hundreds of megawatts and higher [1-5]. The on-line control of delays of the output pulses allows an adjustment of the mutual phasing [5-7] permitting the integral DP scanning in space. Therefore, the accuracy of a time-lock of the microwave sources is required.

The four-channel rf-source is presented below. The external axial magnetic field biased ( $H_z$ ) coaxial nonlinear transmission lines (NLTL) partially filled with ferrite rings were used as the sources of high-power microwave pulses [3-10]. The source rf modulation frequency was increased to 4 GHz, a fairly high output peak power of hundreds of megawatts, and operated at the maximum pulse repetition frequency (PRF) of 1000 Hz.

The microwave oscillations come due to the gyromagnetic phenomena. The gyromagnetic precession excitement takes place under the fast consequent action of a couple of the orthogonal magnetic fields on the magnetic moment of the fully magnetized ferrites. An external bias  $H_z$ -field forms the ferrite saturation in an axial direction, while an incident high-voltage pulse creates an azimuthally magnetic reversal field. As an incident pulse with a sufficient amplitude and rise time propagates through the NLTL, and the sufficient external bias is applied, the ferrite magnetic moments rotate around. The damped gyromagnetic precession excites microwave oscillations.



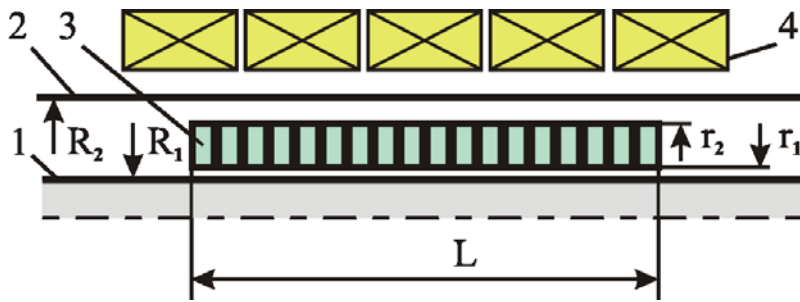


**Figure 1.** Schematic of coaxial NLTL. 1, 2- outer and inner electrode of coaxial line, 3- ferrite rings, 4- solenoid

## 2. Experimental setup

At this work, the two-section NLTLs were used [3, 5-7, 9]. The input section operated as a pulse sharpening device and sharpened a front, sufficient for the second NLTL section operation in the oscillator's mode. Both sections had integrated a construction depicted in figure 1. The ferrite line implements a continuous unit of NiZn-rings of a type M200VNP ( $2R_1=25$  mm;  $2R_2=8$  mm;  $2r_1=10$  mm;  $2r_2=16$  mm) of the total length 700 mm. A direct current solenoid was assembled of five sections, symmetrically placed over a case around ferrite. The NLTL had a partition in the sharpening and generating parts by a self-contained power supply. Experimentally, it has been found that it is optimal to utilize the two first coils for sharpening and delay line tuning of the pulse. The bias field  $H_z$  of the remaining NLTL part was optimized in the range of 35-55 kA/m to form the rf oscillations. The design of NLTL and the biasing field data gave the acceptable delay tuning range (more than the rf half-period), the maximum rf modulation deepness, and the minimized distortion of excited oscillations envelop for a full scale of the delay control.

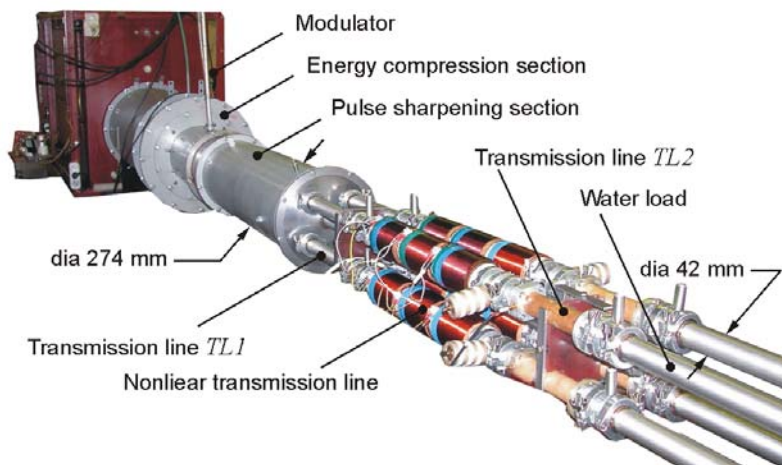


**Figure 2.** A view of the 4-channel rf oscillator on NLTL

The installation view and the basic components of the rf-oscillator are illustrated in figure 2. The full solid state high-voltage driver S500 [11, 12] served as a supply source. The driver formed a pulse with a rise time of  $\sim 1$  ns, the duration (FWHM) of  $\sim 5$  ns, and the amplitude  $V_d \sim 500$  kV in a single pulse mode across a 50 Ohm load. When the system operated at 1000 Hz PRF, the voltage amplitude reduced to  $V_{d1000} \sim 430$  kV.

An output driver pulse was split into four parallel channels by a mismatched cross-type power divider (4x48 Ohm) presented in figure 2. The instability of the pulse amplitude (a total spread 10%, a standard deviation  $\sigma \sim 2\%$ ) was related to the main voltage ripple across a capacitive filter of the primary charging device (PCD).

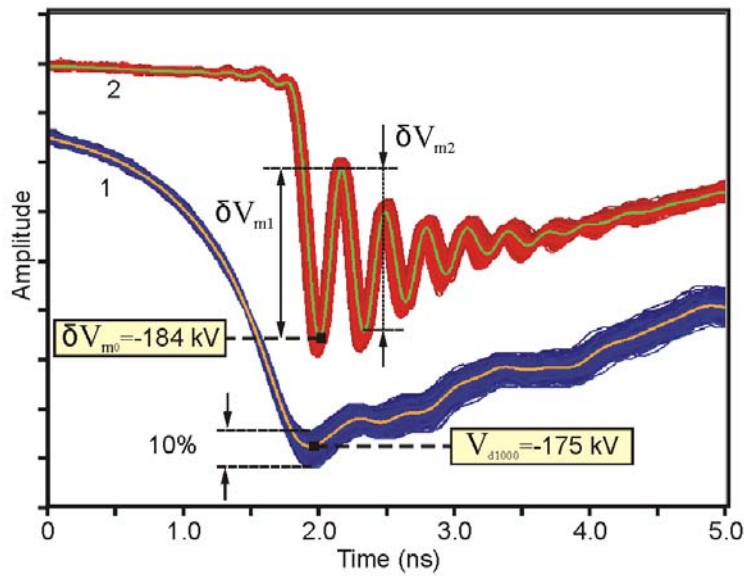


**Figure 3.** Waveforms for a single channel system at repetition rate of 1000 Hz. Pulses of the driver (1) and NLTL (2)

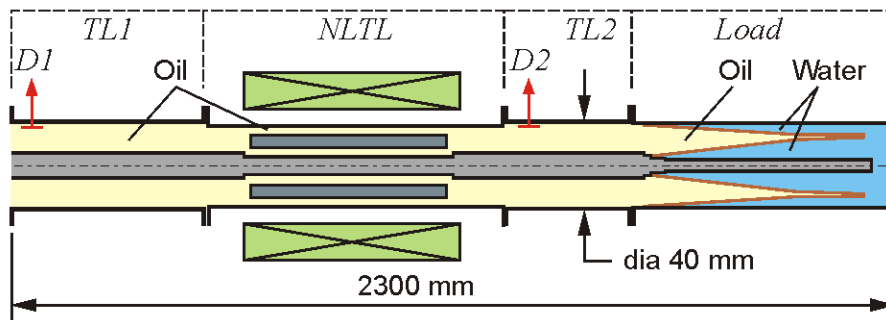


**Figure 4.** Schematic of the NLTL: terminated by a coaxial water line

Every channel was terminated by an absorbing water load (figure 4). The coaxial transition to the water load had a small-angle long conical insulator to minimize the reflections. The voltage pulses were recorded in the oil-filled transmission lines (TL1 and TL2), using the capacitive dividers capable to reproduce  $\sim 70$  ps rise time. The accuracy of amplitude calibration of the dividers D1, D2 was of  $\sim 5\%$ . The location of the dividers in the lines provided about 5 ns delay of the reflected signals.

### 3. Examination of individual NLTL

Testing of the NLTL electric strength and a stability of the output parameters of exited oscillations were held by a single channel terminated by a water line at the repetition frequency 1000 Hz during 1 second. An average input pulse amplitude was  $V_0 \sim 175$  kV, a standard deviation of  $\sigma = 3.5$  kV. An electric strength of the NLTL was enough to operate without breakdown. Waveforms of the output pulse burst are presented in figure 3. The mean value of the first peak of the rf-modulated pulse was  $|V_{m0}| = 184$  kV. An electric field strength on the surface of the NLTL inner electrode of 8 mm achieved  $\sim 425$  kV/cm, and  $\sim 255$  kV/cm in ferrite. An insignificant increase of amplitude due to the shock wave has been formed at the incident pulse front. The maximum increase was obtained by utilizing ferrite rings of the greater diameter [4].

The NLTL excitation mode was chosen so that the modulation depth of the oscillations was maximum after the leading peak ( $V_{m0}$ ). This was achieved by varying the bias field. Varying the solenoid bias field  $H_z$ , the NLTL excitation mode have been adjusted to maximize the modulation depth ( $\delta V_{m1}$ ), which followed the leading peak. The average amplitude and the standard deviation ( $\sigma_0$ ) of the peak ( $V_{m0}$ ), the second peak amplitude ( $\delta V_{m2}$ ), and their ratio to  $V_0$  were measured. The

effective frequencies ( $f_1$ - $f_3$ ) of the three initial peaks were defined as the inversely proportional double time within points at the half-high rise and fall times of the corresponding peaks. The obtained values are listed in table 1.

**Table 1.** Output parameters

Parameters	Value	Parameters	Value	Parameters	Value	Parameters	Value
$ V_{m0} $ , kV	184	$V_{m0}/V_0$ , %	105	$f_1$ , GHz	2.7	$H_z$ , kA/m	55
$ \delta V_{m1} $ , kV	84	$\delta V_{m1}/V_0$ , %	51	$f_2$ , GHz	3		
$ \delta V_{m2} $ , kV	83	$\delta V_{m2}/V_0$ , %	47	$f_3$ , GHz	3.5		

#### 4. High-PRF operation of multi-channel oscillators

The four-channel system was tested to investigate the mutual stability of operation of individual NLTLs under the excitation of rf oscillations. Analysis of obtained results was carried out for a packet of 100 pulses at the pulse repetition frequency of 1000 Hz. The NLTL identity was provided by an equal quantity of the rings and symmetric location of the solenoids over the rings. All channels were terminated by the coaxial water load.

The external bias field of three output coils was identical and was lowered to  $H_{z1}=40$  kA/m. This field gave a maximum delay time turning range and a more sharpened leading peak rise time up to  $t_f=120$  ps. The effective frequency increased to  $\sim 4$  GHz, but the mean value of the output pulse peak amplitude decreased down to -165 kV, figure 5. The output pulse waveforms coincided within a reproduction accuracy of the divider D2 of each channel. The spectrum (the Fast Fourier transformation) of a typical output pulse from the packet is presented in figure 6. The spectrum maximum values (the effective frequency) correspond to  $\sim 4$  GHz.

The channel delay times were various, because the ferrite ring parameters under high voltage, short pulse durations, and the frequency of  $\sim 4$  GHz had not been controlled. The time-lock of a pulse waveform was achieved by current turning in two beginning sections of the solenoid at the output of NLTLs. The identical delays corresponding to calculated fields  $H_{z2}$  generated by the coils were 4; 40; 48, and 57 kA/m.

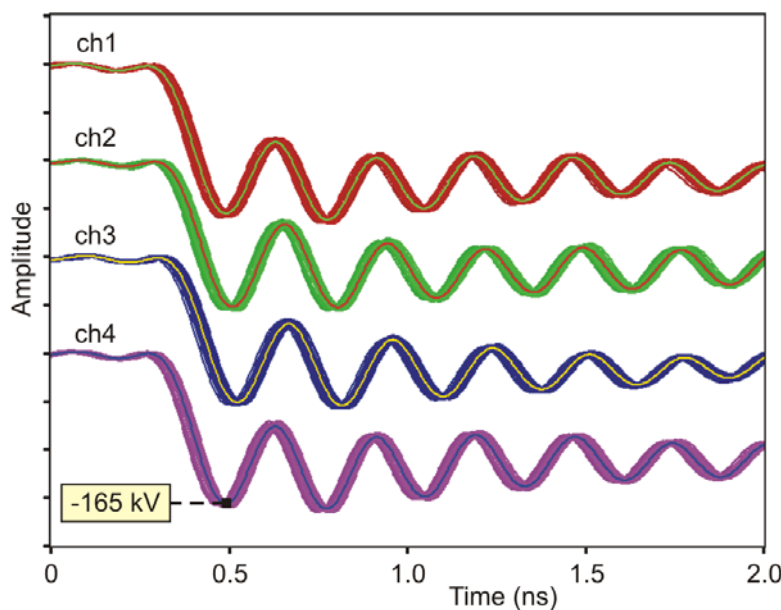


**Figure 5.** Waveforms for a 4-channel systems at repetition rate of 1000 Hz

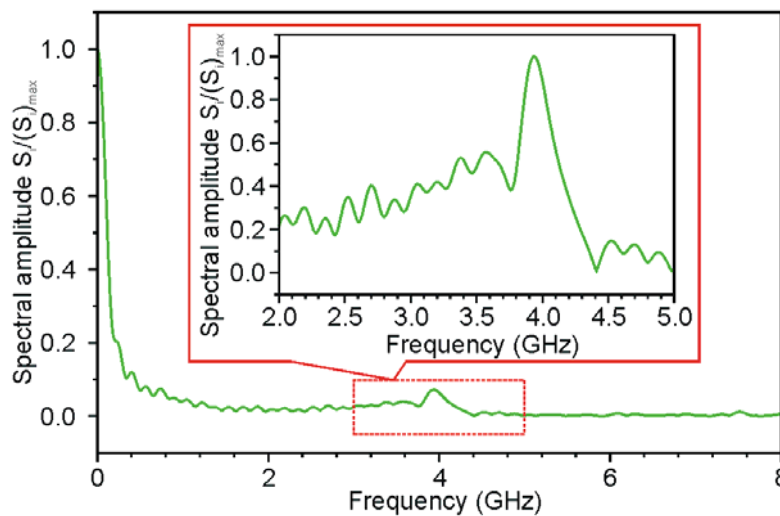


**Figure 6.** FFT spectrums of the output pulse of NLTL

The time instability of generation of the rf-modulated pulses depended on  $H_{z2}$  in the channels. A cross-coupling comparison of the channels showed the maximum relative spread in time-locking of  $\delta t = 55$  ps (15 ps on average) with a standard deviation of  $\sigma_\delta = 20$  ps and had only one channel with a lower minimum  $H_{z2} = 4$  kA/m. The minimum  $\delta t = 35$  ps (8 ps on average) and  $\sigma_\delta = 1.4$  ps were between two channels with sub-equal and high values  $H_{z2}$  40 kA/m и 48 kA/m, which were practically identical to  $H_z$  of the NLTL oscillator section. The decrease in instability with an increasing bias field is predictable, because the deeper ferrite saturation by an external field reduces the ferrite medium state uncertainty in an action of a previous pulse. It is necessary to note, that in the system with the unseparated sharpening and main (gyromagnetic) NLTLs, the channel with  $H_{z2} = 55$  kA/m (in the sharpening NLTL), which is higher than  $H_{z1} = 40$  kA/m (in the main NLTL), had a high  $\sigma_\delta = 9$  ps.

## 5. Conclusions

The designed four-channel rf-source based on a solid-state driver and gyromagnetic NLTLs produced high voltage pulses with a maximum modulation frequency of 4 GHz, with the peak voltage at the NLTL output of 175 kV. The electric strength provided an operation at a pulse repetition rate of 1000 Hz during 1 second. The integral packing of the delay and the modulating sections of NLTLs allowed the electronic time locking. The electronic timing demonstrates the capability of irradiated RF beam steering.

## Acknowledgements

This work was supported by research program of IEP UB RAS 0389-2014-0005 and by RFBR grant No. 16-08-00058.

## References

- [1] Yalandin M I, Shunailov S A, Ul'maskulov M R, Sharypov K A, Shpak V G, Rostov V V, Romanchenko I V, El'chaninov A A, and Klimov A I 2012 *Tech. Phys. Lett.* **38**(10) 917-20
- [2] Sharypov K A, El'chaninov A A, Mesyats G A, Pedos M S, Romanchenko I V, Rostov V V, Rukin S N, Shpak V G, Shunailov S A, Ul'maskulov M R, and Yalandin M I, 2012 *J. Appl. Phys.* **103** 134103
- [3] Rostov V V, El'chaninov A A, Klimov A I, Konev V Y, Romanchenko I V, Sharypov K A, Shunailov S A, Ul'maskulov M R, and Yalandin M I, 2013 *IEEE Trans. On Plasma Sci.* **41** 2735-41
- [4] Ulmaskulov M R, Pedos M S, Rukin S N, Sharypov K A, Shpak V G, Shunailov S A, Yalandin M I, Romanchenko I V, and Rostov V V, 2015 *Rev. of Sci. Instr.* **86** 074702
- [5] Romanchenko I V, Rostov V V, Gunin A V, and Konev V Y, 2015 *J. Appl. Phys.* **117** 214907

- [6] Johnson J M, Reale D V, Krile J T, Garcia R S, Cravey W H, Neuber A A, Dickens J C, Mankowski J J, 2016 *Rev. of Sci. Instr.* **87** 054704
- [7] Johnson J M, Reale D V, Cravey W H, Garcia R S, Barnett D H, Neuber A A, Dickens J C, and Mankowski J J, 2015 *Rev. of Sci. Instr.* **86** 084702
- [8] Bragg J W, Dickens J, and Neuber A, 2013 *J. Appl. Phys.* **113** 064904
- [9] Reale D, Bragg J W, Gonsalves N, Johnson J, Neuber A, Dickens J, and Mankowski J, 2014 *Rev. of Sci. Instr.* **85** 054706
- [10] Romanchenko I V, Rostov V V, Gubanov V P, Stepchenko A S, Gunin A V, and Kurkan I K, 2012 *Rev. of Sci. Instr.* **83** 074705
- [11] Rukin S, Bushlyakov A, Lyubutin S, Ponomarev A, Slovikovsky B, Timoshenkov S, Tsyrarov S, 2007 *Pulsed Power Conference. Digest of Technical Papers. IEEE International* 691-701
- [12] Gusev A I, Pedos M S, Rukin S N, Timoshenkov S P, and Tsyrarov S N, 2015 *Rev. of Sci. Instr.* **86** 114706